16èmes Journées de l'Hydrodynamique

27-29 novembre 2018 - Marseille

SIMULATION NUMERIQUE D'UN SOLITON DEFERLANT AVEC OPENFOAM

J.J. SOUAGA[1], M. BATLLE MARTIN[1], N. HECHT[1], G. PINON[1], J. REVEILLON[2], F.X. DEMOULIN[2]

1 - LOMC - UMR 6294, Normandie Univ, UNIHAVRE, CNRS, 76600 Le Havre.
gregory.pinon@univ-lehavre.fr (* auteur à qui les correspondances doivent être envoyées)

2 - CORIA - UMR 6614, Normandie Univ, UNIROUEN, CNRS, 76801 Saint-Etienne du Rouvray.

Résumé

Dans la suite des travaux de X. Lu [Lu, 2016], l'objectif de ce papier traite de l'impact d'un soliton sur des structures côtieres. L'étude actuelle a été réalisée via le logiciel OpenFOAM, en utilisant une méthode Volume of Fluid resolvant deux phases incompressibles et immiscibles (Solveur interFoam).

Dans une premier partie, nous avons étudié la faisablite d'un tel travail avec le logiciel OpenFOAM. Pour ce faire, le transport et le rebond d'une vague solitaire non deferlante ont été validés. Nous avons vérifié la conservation de l'amplitude de l'onde au cours du temps et comparé nos résultats avec la théorie de Boussinesq. Nous comparons enfin la hauteur d'eau maximale obtenue sur le mur par interFoam avec différentes données analytiques et numeriques.

Dans la seconde partie, l'impact d'une vague solitaire déferlante est traité. Notre souhait étant de trouver les cas d'impacts parmi les plus intenses, nous nous sommes focalisés dans un premier temps sur le cas de "air pocket impact". Ensuite nous avons comparé l'evolution de la surface libre, les formes des vagues lors des impacts et enfin les pressions d'impact avec les resultats expérimentaux de Kimmoun et al. [Kimmoun et al., 2009] et numériques de Lu [Lu, 2016] utilisant la méthode SPH.

Summary

Following the work of X. Lu [Lu, 2016], the objective of this paper deals with the solitary wave impact on coastal structures. This study was carried out numerically via OpenFOAM software, using a Volume of Fluid method to solve two incompressible and immiscible phases (Solver interFoam).

At first, we studied the feasibility of such a work with OpenFOAM software. To do this, the transport and rebound of a non-breaking solitary wave were validated. We verified the wave amplitude conservation over time and compared our results with the Boussinesq theory. Finally, we compare the maximum water height on the wall obtained by interFoam with different analytical and numerical data.

Secondly, the impact of a solitary breaking wave is studied. Due to our aim to find the most intense impact cases, we focused initially on the type "air pocket impact". Then we compared the evolution of the free surface, the wave shapes during the impacts and, to end with, the impact pressures with the experimental results from Kimmoun et al. [Kimmoun et al., 2009] and numeric from Lu [Lu, 2016] using the SPH method.

I – Introduction

Actual climate debate has focused on energy generation and more precisely, on efficiency and feasibility of large device producing clean energy at a national level. This green energy dependency evokes the importance of a diversified and versatile system to fulfill the dynamic population needs. By means of this current, there is a rising part of the population that highlights the great source of clean energy that oceans could provide. The variety of cyclic processes occurring at sea, such as tidal, thermal currents or water waves, makes evident this rising interest.

Nevertheless, these phenomenons may be an opportunity or an issue. In terms of waves, they can cause important damages and losses in the coastlines due to their highly energetic impacts, or conversely, they can be seen as a huge source when looking at their potential energy properties. Therefore, we can take advantage of these two facts together in a technical way by means of installing wave energy devices onto coastal protection structures. Oscillating Water Column (OWC) is a possible concept, protecting the shoreline and generating clean energy at the same time. This engineering structure has been already done in Pico island (Portugal) [13], Mutriku (Spain) [15] or Islay (UK).

These locations have in common severe wave conditions coming from the Atlantic ocean. Therefore, a challenging structural problem is presented in terms of the concrete-reinforced wall (carapace) facing violent water wave impacts such as the vertical wall carapace of Mutriku (see Fig. 1). Thus, the scope of this project is focused on this far discussed coastal engineering phenomenon, which is severe wave impacts on walls.

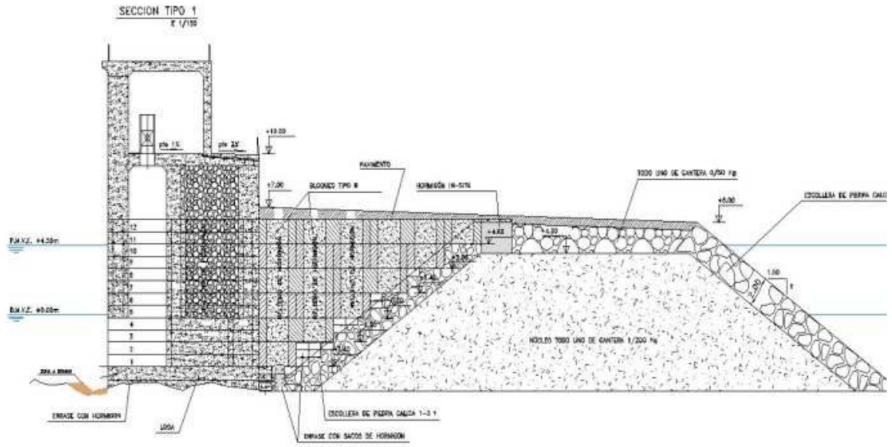

FIGURE 1 – Design scheme of the Mutriku Oscilating Water Column reproduced from Torre-Enciso et al. [15]

The state of art on this topic has been studied experimentally by different authors [1, 5, 7]. Some of them stated the importance of compressibility effects on the evolution of air trapping in plunging waves on the instantaneous significant pressure peaks. Although high sensitivity experiments have been carried out, they presented the difficulties of such configurations. In this scope, water depths and wave heights have a huge impact on wave breaking shape, discrete pressure gauges records and model calibration have high time costs.

Alternatively, numerical methods improve the operative of this circumstances relying on an important initial model calibration. In this scope, Smoothed Particle Hydrodynamics (SPH) models, based on Lagrangian discrete particle methods, have demonstrated good accuracy [4, 9, 10, 14]. One phase simulation of wave impacts outstanding the capacity of this model, nevertheless, the importance of trapped air in the air pocket is obviously related to a two phase model. In this situation, SPH kept demonstrating a good correlation when comparing it with the experiments, even though, it showed to have a high computational cost.

In the other hand, a real time community developed free software, OpenFOAM, is having a huge impact on Computational Fluid Dynamics (CFD). One of its solvers, InterFOAM using Eulerian mesh based with the Finite Volume Method (FVM), makes use of the volume of fluid method to deal with two phase flows. In this scope, two major applications are differentiated depending on our hypothesis of compressible or incompressible flows. Recent studies with this models [11] gave the community a

great source of physical comprehension with acceptable time costs.

To end with, a two-phases 2D numerical wave flume is defined in this paper where a solitary wave will be used to model wave impact. The single event nature of a solitary wave makes it easier to compare it with experiments rather than considering a wave train with many wave-reflections and interactions. The study will deal with wave damping, pressures onto a vertical wall, fundamental aspects of compressibility effects and the comparison of this numerical model with experimental data from Kimmoun et al. [8].

II – The numerical tool : the incompressible InterFoam solver

In this section, the numerical model to solve the two phase problem is briefly introduced. Firstly, InterFOAM equations will be explained under the incompressibility assumptions for both fluids ; this solver will be used in this work.

This finite volume method uses incompresibility assumption coupled with momentum equations to solve the fluid flow in a fixed Cartesian coordinate system. Thus, the Navier-Stokes equations read :

- Mass conservation :

$$\frac{\partial u_i}{\partial x_i} = 0, \tag{1}$$

- Momentum conservation :

$$\frac{\partial \rho u_i}{\partial t} + u_j \frac{\partial \rho u_i}{\partial x_j} = -\frac{\partial p_d}{\partial x_i} - g_j x_j \frac{\partial \rho}{\partial x_i} + \frac{\partial}{\partial x_j}\left[2\mu S_{ij}\right] + \sigma\kappa\frac{\partial \alpha}{\partial x_i}, \tag{2}$$

where u_i are the mean velocity components in a cell, ρ is the density (which will take constant values of ρ_{air} in the air and ρ_{water} in the water), p_d stands for the dynamic pressure ($p_d = p - x_i g_i \rho$), g_j the gravitational acceleration, μ is the dynamic viscosity and S_{ij} represents the mean strain rate tensor given by :

$$S_{ij} = \frac{1}{2}\left(\frac{\partial u_i}{\partial x_j} + \frac{\partial u_j}{\partial x_i}\right). \tag{3}$$

The last term in eq. (2) accounts for the surface tensions effects, where σ is the surface tension coefficient, $\kappa = \nabla \cdot (\nabla\alpha / |\nabla\alpha|)$ is the surface curvature and, finally, α stands for the liquid volume fraction artificial parameter introduced by the volume of fluid method. α takes a value of 0 in the air and 1 in water region. It is defined as

$$\alpha = \frac{\Omega_{water}}{\Omega_{total}} = \frac{\rho - \rho_{air}}{\rho_{water} - \rho_{air}}, \tag{4}$$

where Ω_{water} is the volume of water within a cell and Ω_{total} is the total cell volume. Now any intrinsic fluid property Φ can be defined, such as density or viscosity, by means of α :

$$\Phi = \alpha\Phi_{water} + (1-\alpha)\Phi_{air}. \tag{5}$$

This parameter α is time dependant and must be conserved, thus, the following continuity equation (6) is derived from mass conservation (eq. (1)) :

$$\frac{\partial \alpha}{\partial t} + \frac{\partial \alpha u_i}{\partial x_i} = 0. \tag{6}$$

At this point, InterFOAM aiming to preserve the interface sharpness, an anti-diffusion term is introduced to correct and ensure boundedness. To do so, the MULES solver (Multidimensional Universal Limiter with Explicit Solution) acts on the advective term of eq. (6) adding a correction coefficient as :

$$\frac{\partial \alpha u_i}{\partial x_i} = \int_{\Omega_k} \frac{\partial \alpha u_i}{\partial x_i} dV = \int_{\partial\Omega_k} \alpha u_i n_i dS = \sum_{f \epsilon \partial\Omega_k} (F^L + \lambda_M A)^n, \tag{7}$$

where the Gauss theorem is used to switch from the volume integral to a surface integral. In this equation, n_i is the face normal vector, the superscript n refers to the present time step and, finally, discretizing it for all cell faces f. The last term of eq. (7) stands for face fluxes ; either the flux given

by a low order scheme F^L or the corrected anti-diffusive term $A = F^H - F^L$, where F^H is the flux given by a high order scheme. The limiter λ_M can take values between zero and one in the transition region (interface) and zero elsewhere. This parameter depends on the maximum and the minimum flux a cell can afford in order to maintain α boundedness solution in the next time step. For more details on this implementation, the reader is referred to Santiago et al. [12]. Then, using a pure high order scheme in the interface, the continuity equation becomes :

$$\frac{\partial \alpha}{\partial t} + \frac{\partial \alpha u_i}{\partial x_i} + \frac{\partial}{\partial x_i}\left(\alpha(1-\alpha)u_i^r\right) = 0, \tag{8}$$

where u_i^r is a modelled relative velocity used to compress the interface. Further information could be found in Deshpande et al. [3].

III – Numerical simulations of a non-breaking solitary wave with OpenFOAM

This section is a general overview about a simplified case of a propagating solitary wave according to the Boussinesq theory. The quality of the simulated wave will be assessed through comparisons with the analytic solution in terms of wave elevation, wave shape and run-up.

A test case of a 2D wave channel is chosen to validate the `interFOAM` incompressible solver in a non-breaking solitary wave using the `olaFlow` generation boundary conditions. The case setup will always be a rectangular domain as shown on Fig. 2 with two different phases : water and air. The main aspects in our boundary condition will be, a slip condition at the bottom boundary according to the Boussinesq theory, a `pressureInletOutletVelocity` at the top, where a zero gradient is used except on the tangential component, which has a value of zero, and a `wall` at the outlet.

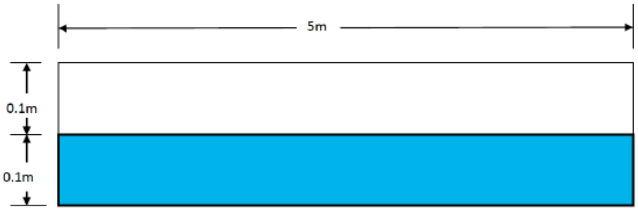

FIGURE 2 – Non-breaking geometry test case

A static wave generator boundary condition will be defined at the inlet. In this work, a solitary wave using the Boussinesq theory will be imposed with a wave height a of $0.025\,m$ for most of the computations. The other geometrical parameters are defined on Fig. 2. This inlet boundary condition defines the liquid volume fraction and velocity fields according to the chosen theory. While the simulation is running, the theoretical wave height (T) is calculated and used to correct the measured (M) using a `fixedValue` zero velocity and a `zeroGradient` α in between levels if (M > T). However, if (T > M) a `waveVelocity` for velocities and a typical `fixedValue` of one for inflow α and `zeroGradient` for outflow, will be used in the interface. For further information, please refer to Higuera et al. [6].

Physical quantity	**Magnitude**	**Unit**
Water density	1000	$kg.m^{-3}$
Air density	1.2	$kg.m^{-3}$
Water kinematic viscosity	10^{-6}	$m^2.s$
Air kinematic viscosity	1.48 x 10^{-5}	$m^2.s$
Surface tension	0.07	$N.m^{-1}$

TABLE 1 – Phases physical properties

The phases physical properties are shown on Table 1. Although, the Boussinesq theory does not take into account the presence of air, nor the effects of viscosity or surface tension ; these physical parameters are natively taken into account in OpenFoam for the presented computations. After comparing the results obtained with different configurations and set up, no effect of these parameters was observed

in the run computations, according to the inertial and gravity predominant physics. Finally, the simulations were run using laminar conditions to compare them with the original Boussinesq theory.

In this section, the results of a solitary wave propagation will be presented and discussed. For all these cases, the physical duration of the simulation was 5 seconds in order to reach the wall situated at the right hand side of Fig. 2. The `writeInterval` was chosen as half a second and used to plot the free surface in space data.

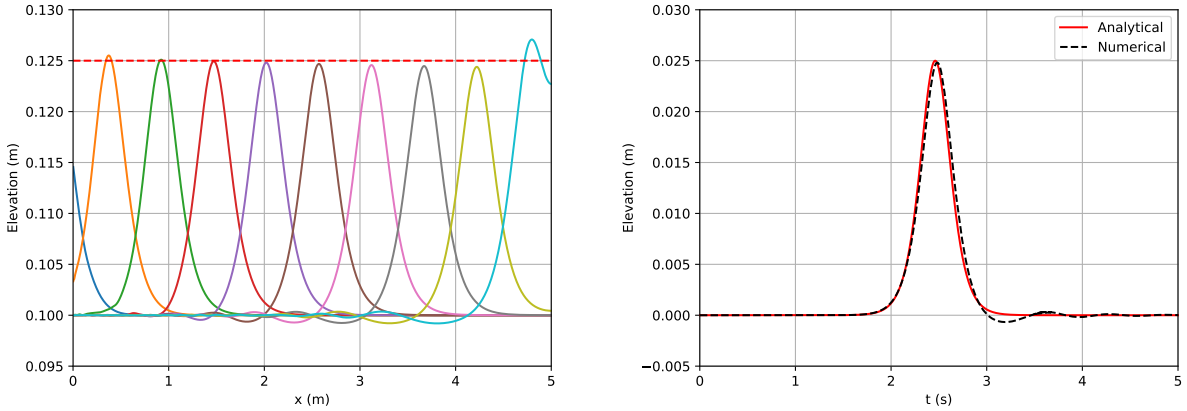

(a) Free surface evolution every 0.5s.

(b) Analytic comparison

FIGURE 3 – Free surface evolution every $\Delta t = 0.5s$ and numerical free surface comparison using the Boussinesq theory two meters from the inlet boundary condition

To begin with, the propagation in space of the solitary wave is presented in Fig. 3(a). Here, the red dashed line represents the input amplitude and, the continuous lines, the obtained free-surface referenced to a write interval data. One can observe that, the first curve referred to $0.5\,s$ is not fully observable on the domain due to the time lag chosen to generate the wave. The following discussion focuses after the second curve, since this is still to close to the inlet boundary, where a maximum wave amplitude damping of around 0.8% per meter was observed. Finally, the last curve shows the run-up due to the interaction with the wall.

Figure 3(b) compares the analytic and the numerical solution. Numerical data was extracted from a gauge located two meters away from the wave-maker, far enough considering the equivalent wave length for our solitary wave around 1.45 m, where at every computation time step the free surface was calculated using the ratio between the volume of water and the total volume. In this situation, the numerical approach has important similarities with the analytic function in terms of shape and wave parameters. Although, as noticed in the spatial study, a diminution of the maximum wave height is appreciable with an error of 0.7% calculated as

$$\Delta E = \left| \frac{\phi_{numeric} - \phi_{analytical}}{\phi_{analytical}} \right|, \tag{9}$$

ϕ being the studied field. Furthermore, time lag is noticeable when looking at the wave crests of 0.02 s and, finally, some residual waves of low amplitude appear after the event probably produced by the wave maker due to the infinite wave length assumption.

After validating the energy conservation with Fig. 3(a), the free surface shape with respect to analytic solution with Fig. 3(b), Figure. 4(a) is devoted to a grid convergence analysis of the software. Three different mesh discretisations were considered. It can be observed that the obtained free surfaces, even close to the opposite wall, meaning that the solitary waves traveled since generation are nearly superimposed whatever the discretisation is. In that respect, the used computations could be considered as converged. Finally, to complete this non-breaking configuration with some physical analysis, the maximum run-up H_{max} on the opposite wall is presented in Fig. 4(b). Such comparisons were already performed in the work of Lu [9] where the SPH numerical results are also presented together with the linear theory and the results from Byatt-Smith et al. [2]. It can be observed on this Figure 4(b) that the obtained results really fit with the linear theory for small relative wave amplitudes

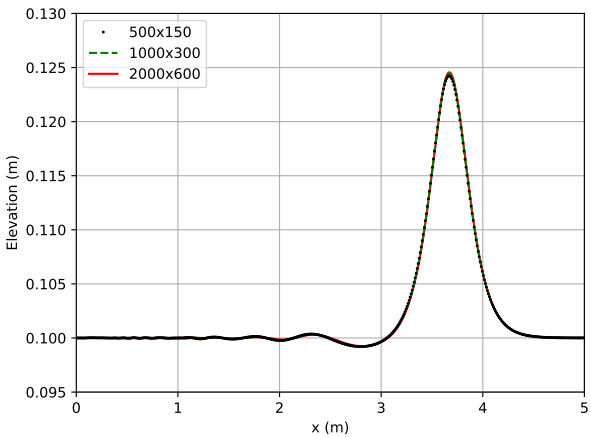

(a) Mesh convergence analysis

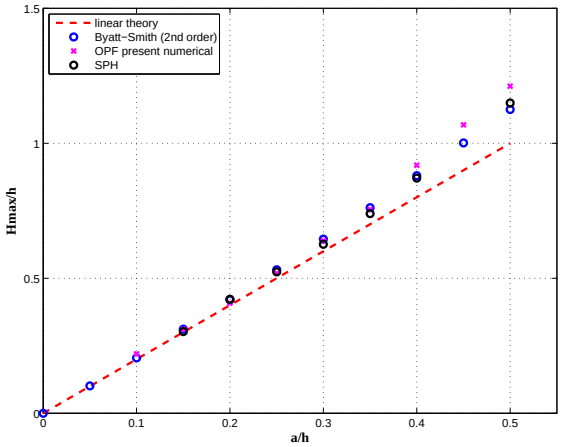

(b) H_{max}/h

FIGURE 4

a/h. Increasing this relative amplitude makes the results slightly move aside from the linear theory from $a/h \gtrsim 0.3$ but this behaviour is completely coherent with physical phenomenon and also with the former results of Lu [9] and Byatt-Smith et al. [2]. However, for the larger amplitudes, the present OpenFoam results tend to show higher no-linear effects than the two pre-cited references. This aspect will need further investigation.

IV – Numerical computations of a breaking solitary wave impinging a wall

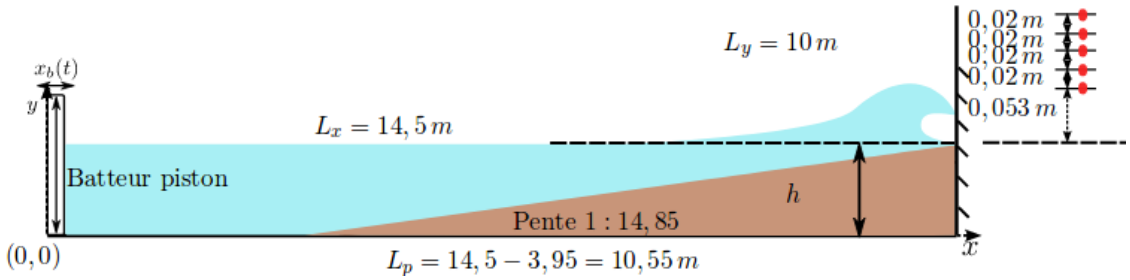

FIGURE 5 – Geometrical configuration of the reproduced experimental configuration of Kimmoun et al. [8]

As it was already studied in the work of Lu [9], the solitary wave breaking case is under review in the present work to compare both SPH and OpenFoam performances on a similar configuration. The reproduced experimental configuration presented on Fig. 5 and taken from the experimental work of Kimmoun et al. [8] will now be treated with the interFoam solver. Among the main advantages of these experiments is that several pressure probes were installed flush on the impacted wall for different wave configurations. These pressure records will be of great interest in the last paragraphs of this section.

Before comparing the pressure records, some validations needed to be performed to make sure that the breaking wave was similar to the experimental one. First, a temporal free surface elevation at $x = 2.8\,m$ from the wave-maker obtained from a numerical wave gauge is compared with analytic (Boussinesq) and experimental [8] results. The main physical and numerical parameters are $h = 0.716\,m$, $a = 0.0864\,m$ and $dx = dy = 0.018\,m$. These results show a fairly good accordance between the analytic and experimental results on the solitary wave shape, whereas the numerically obtained free surface is slightly larger in width. However, all the three results nearly exactly coincide on the soliton amplitude. Finally, for the experimental and numerical cases, the free surface does not recover a still state after the passing of the solitary wave. This aspect could be attributed to the fact that, in both cases cases, the infinite wave length cannot be exactly reproduced neither numerically nor experimentally. However, a general good accordance of the results are obtained.

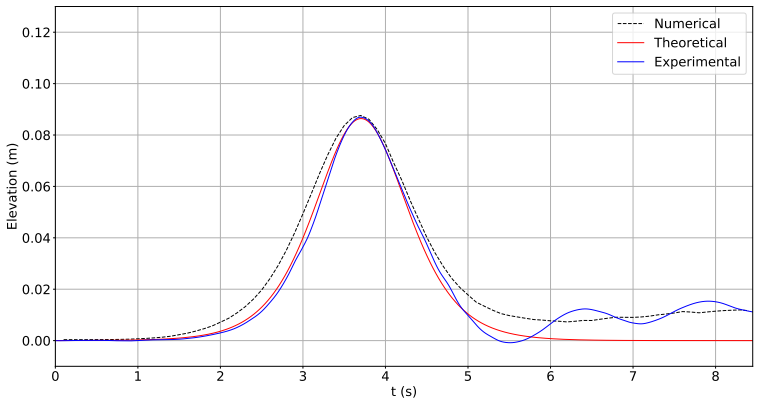

FIGURE 6 – Temporal free surface elevation at $x = 2.8\,m$ from the wave-maker obtained from a numerical wave gauge ($h = 0.716\,m$, $a = 0.0864\,m$ and $dx = dy = 0.018\,m$) compared with analytic (Boussinesq) and experimental results [8].

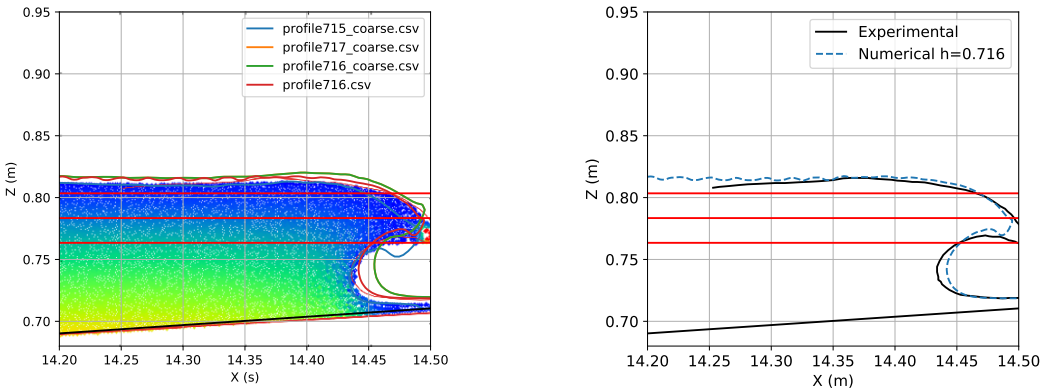

(a) Free surface comparison with Lu [9].

(b) Free surface comparison with experiments

FIGURE 7 – Comparisons of the breaking wave shapes just before impact for different meshes ($dx = dy \approx 0.036\,m$ and $dx = dy = 0.018\,m$) and water depths.

Both graphs of Figure 7 depict the breaking wave shapes just before impact for different meshes and water depths. In the presented numerical results, $\alpha = 0.5$ is used to represent the free surface. Comparison is also made with the SPH numerical results of Lu [9] and the experimental results of Kimmoun et al. [8]. In both experimental and numerical configurations, the solitary wave amplitude is $a = 0.0864\,m$ whereas different numerical water depths are considered in order to more accurately reproduce the breaking wave shape just before impact. The best correspondence with the experimental wave breaking shape is obtained here for a water depth value of $h = 0.716\,m$ with respect to the experimental value $h = 0.7185\,m$, that is to say a difference at the order of two millimeters or less. This numerical configuration with $h = 0.716\,m$, $a = 0.0864\,m$ and $dx = dy = 0.018\,m$ will be used in the following to compare the pressure records and do some physical analysis.

The horizontal red lines of Fig. 7 represent the pressure probes altitudes where the pressure records will be made on the opposite wall. These experimental pressure records at three altitudes (namely $0.053\,m$, $0.073\,m$ and $0.093\,m$ above the sloped plane) are presented in Figure 8 with the numerically obtained pressure records. For the numerical results, the record at the exact position plus additional two (just above and lower $+/-0.005\,m$) are depicted as a matter of comparison. Several conclusions can be drawn. First the general values of the pressure is correct and maximum values at the order of $\approx 180\,mbar$ are numerically reproduced. More into details, for the middle probe ($0.073\,m$ above the sloped plane) which is very interesting physically, the first short impact peak is somehow reproduced in intensity ($\approx 180\,mbar$) shape and duration ($\approx 0.0025\,s$). However, as openFoam is slightly more

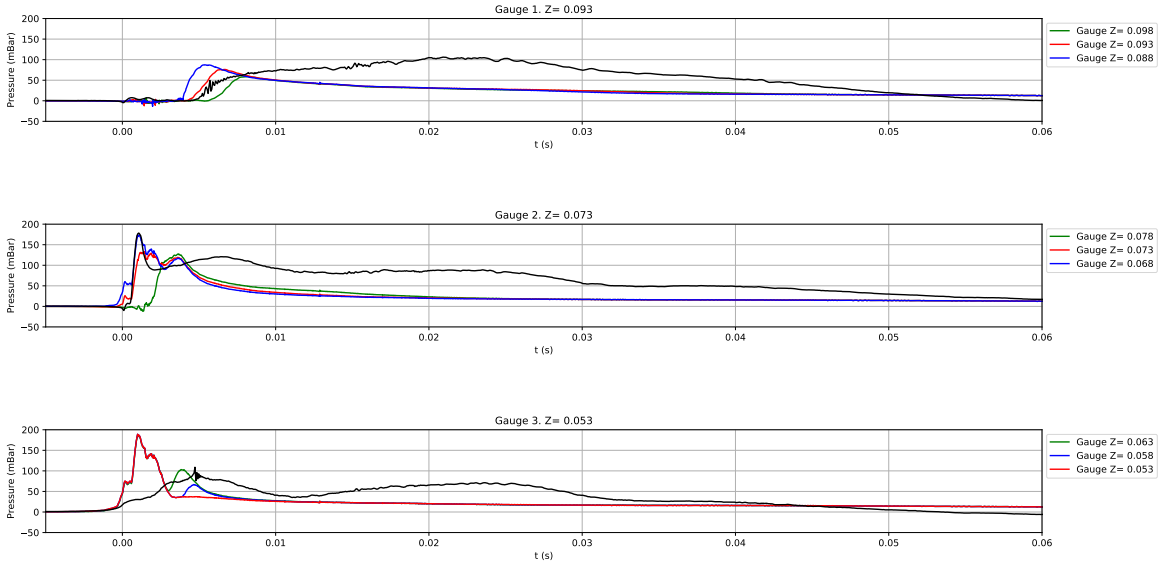

FIGURE 8 – Pressure history for $h = 0.716\,m$ at different gauges. Sub-titles refer to the experimental values here in black lines. Time lag was adjusted and the other parameters are $a = 0.0864\,m$ and $dx = dy = 0.018\,m$.

diffusive than SPH for instance, the very sharp increase from atmospheric pressure the the maximal value is not exactly reproduced numerically. The present numerical results are slightly smoothed with respect to the experiments. Then, the second at approximately $t = 0.005 - 0.006\,s$ with a value of $\approx 120\,mbar$ also exists numerically but its duration is shorter together with a time shift. This second pressure peak, also experimentally observable on the lower probe ($0.053\,m$ above the still water level) is physically due to the air entrapment by the breaking wave. In the presented computations, as the computations are 2D and incompressible, the pressure in the entrapped air pocket tends to instantaneously adjust to the maximum pressure of the water impact one, that is to say at $\approx 180\,mbar$ (see Fig. 9(a) for instance). Experimentally, this is absolutely not the case as the experiments are 3D and, even though the wave profile is mainly 2D, some gaps existed on the sides of the wall in the experimental configuration to enable the wall to move in some cases. Therefore, the experimental maximum pressure value at $\approx 100\,mbar$ is much smaller than the numerical one for the lower probe and the pressure record are also different.

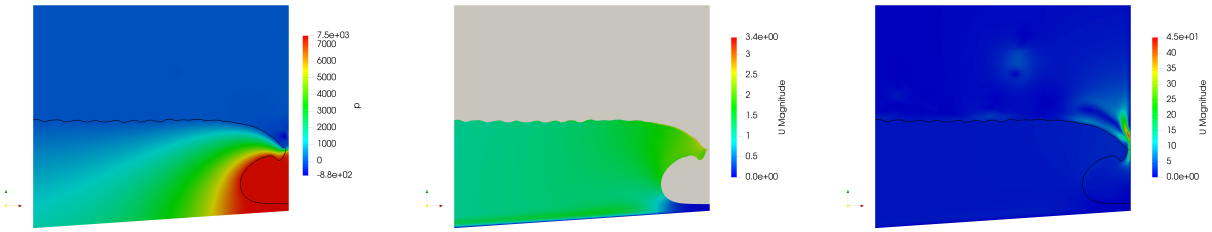

(a) Pressure (b) Water velocity (c) Air velocity

FIGURE 9 – Total pressure - water and air velocity magnitudes at the same time just before impact for $h = 0.716\,m$, $a = 0.0864\,m$ and $dx = dy = 0.018\,m$ using a refined non graded mesh.

Many more physical interpretations and numerical experimental comparisons could be done. One of the last could be the intense air velocities numerically observed just above the breaking wave on Fig. 9(c). Again, this is mainly due to the considered 2D configuration for the numerical computations, a phenomenon that might not be observed in the real 3D experimental configuration. But all these aspect will need further investigation in a near future.

V – Conclusion

To conclude, this work is the continuation of a previous study carried out by Lu [9]. The previously obtained results using the SPH approach were already very promising in terms of soliton propagation accuracy and impact pressure predictions, although some major improvements needed to be done. One of them was the use of a two-phase software. Such two-phase computations were also run in Lu [9] but the computations costs were very high. Therefore, this study is a new attempt to treat this wave impact problem using the open source code OpenFoam. A similar approach comparing first non-breaking configurations with the theory and some experiments to evaluate the wave propagation properties, the solitary wave rebound and run-up, gave concluding results. In a second step, breaking configurations similar to the experimental configuration of Kimmoun et al. [8] were tempted. A single case ($a = 0.0864\,m$ and $h = 0.7185\,m$) was treated in the present paper, corresponding the the air pocket impact already studied by Lu [9]. The obtained computations gave interesting results in terms of wave shape before impact and impact pressures measured on numerical pressure probes mounted flush on the wall. Comparisons of these above-mentioned results with the experimental ones of Kimmoun et al. [8] also show some discrepancies. However, some interesting physical interpretations can be already observed from the computations and will be presented during the conference presentation.

To further improve the results, both the use of a 3D incompressible or 2D/3D compressible approach are considered. However, these computations will have a increase in terms of CPU resources that need to be quantified. Also, different wave amplitudes and water levels as those used in the paper were studied experimentally and such cases could also be an interesting path to investigate.

VI – Acknowledgements

The authors acknowledge the financial support of the French Agence Nationale de la Recherche (ANR), through the program "Investissements d avenir"(ANR-10-LABX-09-01), LabEx EMC3. The authors also would like to acknowledge the support of the European and Regional Fundings called Neptune and Semarin, the last supporting the post-doc grant of N. Hecht. Finally, Marc Batlle Martin would like to thank the Normandy regional council for the funding of his PhD grant. This work was granted access to the HPC resources of CRIANN (Centre Régional Informatique et d'Applications Numériques de Normandie).

Références

[1] G. Bullock, C. Obhrai, D. Peregrine, and H. Bredmose. Violent breaking wave impacts. part 1 : Results from large-scale regular wave tests on vertical and sloping walls. *Coastal Engineering*, 54(8) :602 – 617, 2007.

[2] J. G. Byatt-Smith. An integral equation for unsteady surface waves and a comment on the boussinesq equation. *Journal of Fluid Mechanics*, 49(04) :625–633, 1971.

[3] S. Deshpande, L. Anumolu, and M. F. Trujillo. Evaluating the performance of the two-phase flow solver interfoam. 5, 11 2012.

[4] P. Guilcher, G. Oger, L. Brosset, E. Jacquin, N. Grenier, and D. Le Touzé. Simulation of liquid impacts with a two-phase parallel SPH model. In *Proceedings of 20th International Offshore and Polar Engineering Conference, June 20-26, Bejing, China*, 2010.

[5] M. Hattori, A. Arami, and T. Yui. Wave impact pressure on vertical walls under breaking waves of various types. *Coastal Engineering*, 22(1) :79 – 114, 1994. Special Issue Vertical Breakwaters.

[6] P. Higuera, J. Lara, and I. Losada. Realistic wave generation and active wave absorption for navier-stokes models application to openfoam (r). 71 :102–118, 01 2013.

[7] B. Hofland, M. Kaminski, and G. Wolters. Large scale wave impacts on a vertical wall. *Coastal Engineering Proceedings*, 1(32) :structures–15, 2011.

[8] O. Kimmoun, Y. Scolan, S. Malenica, et al. Fluid structure interactions occuring at a flexible vertical wall impacted by a breaking wave. In *The Nineteenth International Offshore and Polar Engineering Conference*. International Society of Offshore and Polar Engineers, 2009.

[9] X. Lu. *Simulations numériques de l'action de la houle sur des ouvrages marins dans des conditions hydrodynamiques sévères*. PhD thesis, Normandie Université, 2016. Thèse de doctorat.

[10] X. Z. Lu, J.-M. Cherfils, G. Pinon, E. Rivoalen, and J. Brossard. SPH Numerical computations of wave impact onto a vertical wall. In *9th international SPHERIC workshop*, June 2014. Paris, France.

[11] Z. Ma, D. Causon, L. Qian, C. Mingham, and P. M. Ferrer. Numerical investigation of air enclosed wave impacts in a depressurised tank. *Ocean Engineering*, 123 :15 – 27, 2016.

[12] S. Márquez Damián. *An Extended Mixture Model for the Simultaneous Treatment of Short and Long Scale Interfaces*. PhD thesis, 03 2013.

[13] F. Neumann and I. L. Crom. Pico owc - the frog prince of wave energy ? recent autonomous operational experience and plans for an open real-sea test centre in semi-controlled environment. In *9th European Wave and Tidal Energy Conference (EWTEC)*, 5-9 Sep. 2011 2011. Southampton, UK.

[14] G. Oger, P. Guilcher, E. Jacquin, L. Brosset, J. Deuff, D. Le Touzé, et al. Simulations of hydroelastic impacts using a parallel SPH model. *International Journal of Offshore and Polar Engineering*, 20(3) :181–189, 2010.

[15] Y.Torre-Enciso, I.Ortubia, L. L. de Aguileta, and J. Marqués. Mutriku wave power plant : from the thinking out to the reality. In *8th European Wave and Tidal Energy Conference (EWTEC)*, September 2009. Uppsala, Sweden.